Hindawi
Mathematical Problems in Engineering
Volume 2022, Article ID 6462085, 15 pages
https://doi.org/10.1155/2022/6462085

Research Article

An Adaptive Nonsingular Fast Terminal Sliding Mode Controller for Dynamic Walking of a 5-Link Planar Biped Robot in Both Single and Double Support Phases

Ataollah Azarbani, Mohammad Bagher Menhaj, and Ahmad Fakharian

Faculty of Electrical, Biomedical and Mechatronics Engineering, Qazvin Branch, Islamic Azad University, Qazvin, Iran

Correspondence should be addressed to Ahmad Fakharian; ahmad.fakharian@qiau.ac.ir

Received 6 November 2021; Accepted 13 January 2022; Published 4 February 2022

Academic Editor: Le Anh Tuan

This paper aims to design an improved adaptive nonsingular fast terminal sliding mode controller for a fully actuated planar biped robot with five degrees of freedom in the single support (SSP) and double support (DSP) phases in the presence of external perturbation and uncertainties. A new sliding surface was proposed to avoid singularities and the chattering phenomenon. The proposed controller guarantees fast convergence of error signals in finite time. Unlike similar studies, the presented method considers a whole cycle of one step of walking, including SSP, double impact, and DSP phases. Also, the proposed approach does not require a predefined upper limit to estimate uncertainty using an adaptive law. Notably, dynamic walking was preferred over static walking to achieve more similarity to human walking. The designed trajectories were determined according to the position of the waist and swinging legs ankle, which could then be converted into the position of joints using inverse kinematics equations. The simulation results were used to approve the proposed controller's fast and robust tracking performance in the presence of external disturbances, mass, and inertia uncertainties without predefined knowledge of their upper bounds.

1. Introduction

Biped robot control has attracted considerable attention in the last two decades. Compared to mobile and manipulator robots, these robots are tough to control due to inherent instability and dependence on balance and motion control systems. Biped robots also have several advantages: easier negotiation on discrete surfaces, such as stairs, rough, and uneven surfaces, and stepping over obstacles. Biped robots are typically controlled by controllers with specific characteristics. However, uncertainty in robot types and external perturbations, such as sudden forces applied to the robot or overweight and carrying cargo, have degraded the performance of such control systems. Therefore, robust and adaptive controllers have been considered in this regard. In [1], the application of sliding mode control in motion control systems has been reviewed. This method has been investigated in continuous-time and discrete-time systems and high-order forms. A new second-order sliding mode control has been provided in [2], which employed a definite function instead of an upper bound for a constant uncertainty. Regarding this change, a closed-loop system was globally stable and had global finite-time stability. Simulation results for multiple numerical examples demonstrated a suitable performance for this method. The sliding mode controller was combined with the extended state observer (ESO) in [3] to control pneumatic artificial muscles in the presence of perturbation. The design of ESO has compensated for the effect of differences among the model and real system, system uncertainties of the model, and external perturbations. The Lyapunov theory guarantees the convergence of observer and closed-loop stability of the system. The simulation and practical implementation of this method on a muscle with two joints proved its effectiveness.

In [4], the second-order terminal sliding mode method has been introduced to control linear systems in the presence

of uncertainty. The method confirmed more accurate tracking and fast convergence to the reference trajectory with no chattering in that study. Simulation of some numerical examples demonstrated accepted effectiveness. The terminal sliding mode controller was used to control a manipulator robot [5]. Unlike conventional methods, this innovative approach involved a finite-time convergence to zero for the tracking error, ruling out the need for an explicit use of system dynamical model. This method has proved effective by simulating a manipulator robot with two degrees of freedom.

In [6], the finite-time sliding mode controller has been used to track reference trajectories of a manipulator robot with two degrees of freedom. The simulation and practical implementation results have indicated its good performance in the presence of external perturbations with no need for additional compensation. A super twisting sliding mode controller was introduced in [7] as a finite-time system to track reference trajectories of a manipulator robot. This method does not need to explicitly use the robot's complicated model or estimate uncertainties and unmodeled dynamics of the robot. The conventional super twisting method includes an unknown nonlinear function that should be classified into two definite and indefinite categories being hard to perform. The present paper has solved this problem by designing a proper adaptive law for the unknown function. Simulation on a manipulator robot with two joints easily approved the method's efficacy: a second-order fast terminal sliding mode controller was proposed in [8] for a class of nonlinear systems in the presence of uncertainty. The proposed controller was designed using the Lyapunov theory and the linear matrix inequalities (LMI) in the present study. This designed controller does not depend on model order. It can be easily employed for systems with higher and more complicated orders. The simulation in Chua and Genesio chaotic systems showed this method's satisfactory performance.

The adaptive sliding mode control (ASMC) approach was reviewed in [9]. Various types of divergence, including uniformly ultimate boundedness, asymptotically, and finite-time, were provided to design ASMC. The characteristics of each have then been discussed. In [10, 11], a new ASMC was designed by introducing an integral/exponential adaptation law to reduce chattering and enhance the controller's performance. The sufficient and the required conditions for the proposed controller were also investigated. In [12], the ASMC approach was used to control the position and attitude of a quadrotor with six degrees of freedom. The closed-loop uniformly ultimately stability was also confirmed by the Lyapunov theory. Simulations demonstrated the suitable performance of this method in the presence of uncertainties and external perturbations.

In [13], a sliding mode controller was designed with one adaptive control law without requiring the upper bound of uncertainty and perturbation information. This method was simulated on an electropneumatic actuator. In [14], ASMC has been proposed for unknown nonlinear systems. This method needed no predetermined information about uncertainty bounds. The simulation on a manipulated robot with two degrees of freedom approved the performance. ASMC with no need for a priori bounded uncertainty was designed in [15], which was simulated on the general class of Euler-Lagrange systems.

A terminal sliding mode controller was designed to control a class of nonlinear systems in the presence of uncertainty and perturbation [16]. The perturbation was estimated via an adaptive sliding mode disturbance observer. The subject control law was continuous-time and nonsingular, and stability was provided in the finite-time form. Simulation results exhibited its better performance compared to the conventional sliding mode. In [17], a fast nonsingular terminal sliding mode control with an adaptive law was employed to estimate the boundaries of uncertainties. This method did not need a priori disturbance. Results of simulation on a flexible spacecraft represented proper efficacy compared to other related methods. A fast nonsingular terminal sliding mode control was proposed in [18] to track reference trajectories in mobile robots in the presence of external perturbations and uncertainties.

In [19], the ASMC method was used to control a manipulator robot in the high-order super twisting sliding mode. The results indicated fast adoption and finite-time convergence. The adaptive nonsingular fast terminal sliding mode control was designed in [20] to track reference trajectories for a manipulator robot in the presence of uncertainty and external perturbations. The suitable adaptation law designed for this method ensured a fast and finite-time convergence while avoiding singularity. This method needed no information about the upper limit of uncertainty and perturbation. These values were estimated via an adoption law using measured positions and velocities of the robot. In [21], the adaptive second-order fast nonsingular terminal sliding mode was introduced to control the manipulator robot in the presence of uncertainty and external perturbation. No data about the upper bound of uncertainty was needed. The uncertainty could be estimated online using an appropriate adoption law. An adaptive nonsingular fast terminal sliding mode control was proposed in [22] to track reference trajectories of an underactuated quadrotor. An adaptive integral sliding mode approach was used in [23] to control underactuated autonomous underwater vehicles in the presence of uncertainty. This method uses radial basis function (RBF) neural networks to estimate the upper limit for perturbation and uncertainty.

The researchers proposed an adaptive super twisting terminal mode controller [24] for a particular class of fourth-order systems, in which the upper bound of external perturbations can be obtained using a proper adoption law. This method's simulation and practical implementation on a cart-pol system demonstrated better performance than other available methods. An adaptive super twisting terminal mode controller was utilized in [25] to control a manipulator robot with two degrees of freedom. In [26], the ASMC method was used to control manipulator robots considering time delay. In this regard, the time delay was estimated, and uniformly ultimately bounded stability was guaranteed by fast-tracking but negligible chattering. This method's simulation and practical implementation represented better

performance than the conventional ASMC method. In [27], ASMC was proposed to control unknown nonlinear systems in the presence of variable time delay at the input. The control efficacy of this method can be determined using LMI. In [28], a back-stepping integral sliding mode controller was suggested for quadrotor UAVs using iterative learning algorithms. Also, trajectory tracking was proposed for quadrotor UAVs considering the payload [29]. In [30], a robust mixed H_2/H_∞ with a fuzzy approach was utilized for robot manipulators. Moreover, in [31–33], an adaptive fast nonsingular terminal sliding mode control was used for autonomous underwater vehicles (AUVs) and unmanned underwater vehicles (UUVs).

There are many studies about biped robots concerning sliding mode control. In [34], the sliding mode approach was adopted to control a biped robot with five degrees of freedom in the presence of uncertainty in both SSP and DSP states. This controller was also designed in [35] for an underactuated biped robot with five degrees of freedom. In [36], a biped robot with five degrees of freedom was controlled only in the DSP state using the sliding mode control. A biped robot was also controlled in [37] using the sliding mode control. They managed to remove chattering by an innovative method. Simulation results showed robustness against both uncertainties and external perturbations. In [38], an adaptive super-twisting nonsingular terminal sliding mode approach is utilized to control the attitude and latitude of aircraft. However, note that the mentioned method dose does not produce chattering-free signals. An adaptive robust recursive SMC was presented in [39] for attitude control of a quadrotor. In their method, a two-layer sliding surface was introduced with an integral sliding surface and a fast terminal nonsingular one. The complexity and volume of calculation were costly, and the chattering phenomenon was not wholly removed.

The present paper has developed an adaptive nonsingular fast terminal sliding mode controller for a planar biped robot with five degrees of freedom. The main novelty of this paper is fast convergence without chattering for multi-dynamic systems, even switching dynamics. It was made by combining the nonsingular fast terminal sliding mode and a new higher-order sliding mode surface. Furthermore, in the proposed method, the discontinuous term (sign function) was placed in the time derivative of the control input. Thus, there was no discontinuous term in control input and no chattering in tracking error signal. Moreover, the proposed method did not consider the upper bound of uncertainties predetermined. The suggested adaptive control law estimated the unknown uncertainties without knowing the upper limit of uncertainties and external perturbation. Unlike similar studies, the proposed method considers a whole cycle of one step of walking, including SSP, double impact, and DSP phases, to make the obtained model approximate to actual human walking. It has been assumed that the proposed robot walks dynamically, and perturbation is applied to the trunk in the form of overloading. Given the essential instability in biped robots' dynamic walking and smooth movement, it is vital to produce chatter-free signals as fast as possible. Meanwhile, the robot should avoid the singularity problem. Unlike some references using the boundary cortex approaches to reduce or remove the chattering phenomenon at the cost of demeaning system robustness (reviewed in the introduction), in this study, the discontinuous part (sign function) is involved in the time derivative of the suggested control signal. Hence, the real control law after integral is continuous; therefore, the signals have no chattering without touching the tracking performance.

The designed reference trajectories were determined based on the dynamical stability of the robot based on the position of waist and ankle of the swinging leg at both SSP and DSP states. They were converted into the joints' position using inverse kinematics equations. The reference trajectories are designed as well in order to always keep zero moment point (ZMP) in a stable region. Thus, ZMP has always been placed in the support polygon of the robot with respect to dynamical stability confirmation. This designed controller has been able to track reference trajectories of robot joints at both SSP and DSP phase with a proper and fast convergence velocity, without chattering and in a robust manner, even while velocities are suddenly changed in transition from SSP to DSP dynamics. Based on the designed adoption law, the proposed method does not require knowing the upper limit of uncertainty as a predetermined value, which can be estimated online. Using a new sliding surface and developing a new control inputs definition, fast convergence in finite time with avoidance singularities and chattering behavior is guaranteed. The simulation results easily approved an appropriate performance for the proposed method in dynamic walking of robot in the presence of uncertainty and external perturbation. Despite its many advantages, the proposed method has a larger computational volume than a similar non-adaptive method. Nonetheless, this approach is less complicated than methods using different observers to estimate unknown terms (disturbance or uncertainty) with unknown upper bounds.

In this paper, Section 2 discusses the dynamics of a biped robot involving SSP, DSP, and double impact phases. Section 3 examines motion planning. Section 4 describes the design of an adaptive nonsingular fast terminal sliding mode controller in detail. The simulation results have been provided and analyzed in Section 5. Finally, Section 6 presents the conclusions.

2. Biped Robot Dynamics

The characteristics of human motion are mostly expressible in a five-link planar robot. The selected robot has minimum degrees of freedom and can excellently simulate humanized behaviors. The five-link robot contains one trunk with two legs, each leg containing thigh and shank. Assuming a low mass for the link of feet, the degree of freedom will not increase. The main task of feet is to apply torque at the ankles area, exert a force to detach the heel, and play a supportive role during the motion. The mass-free link for feet makes it possible to insert the torque applied to the ankle of the supporting leg into the dynamics. The force for detaching the leg from the ground at feet can also be

modeled with the sudden force or forces constrained to tips. The intended five-link robot in this study contained two thighs and two shanks, and two mass-free links for feet. The robot comprised a joint at hips, two joints at knees, and two joints at ankles. Each joint has a torque actuator. All joints could only rotate on the lateral plane at the DSP state. The torque was only implemented in the front ankle, and the rear ankle could rotate freely. It was assumed that the torque between feet and the ground sufficed to prevent slippage during walking [40–43]. Figure 1 illustrates the schematic representation of the robot.

To achieve kinematics, the biped robot was considered as open-loop chained links with the starting point from the supporting leg and ending at a free point, similar to a manipulator robot. In this regard, the kinematics and dynamics equations of the robot were simplified, and the computation time was reduced. The position and velocity of the swinging tip were obtained from the following equations considering Figure 1:

$$\begin{aligned} x_e &= x_b + l_1 \sin\theta_1 + l_2 \sin\theta_2 + l_4 \sin\theta_4 + l_5 \sin\theta_5, \\ y_e &= y_b + l_1 \cos\theta_1 + l_2 \cos\theta_2 + l_4 \cos\theta_4 + l_5 \cos\theta_5, \\ \dot{x}_e &= l_1 \cos\theta_1\dot{\theta}_1 + l_2 \cos\theta_2\dot{\theta}_2 + l_4 \cos\theta_4\dot{\theta}_4 + l_5 \cos\theta_5\dot{\theta}_5, \\ \dot{y}_e &= -l_1 \sin\theta_1\dot{\theta}_1 - l_2 \sin\theta_2\dot{\theta}_2 + l_4 \sin\theta_4\dot{\theta}_4 + l_5 \sin\theta_5\dot{\theta}_5, \end{aligned} \tag{1}$$

where m_i and l_i stand for mass and length of the link i, d_i is the distance between center of mass of the link i to the joint i, I_i is the inertia of the link i around an axis passes through center of mass of the link i perpendicular to the lateral plane, and θ_i is the angle of the link i with the vertical axis. (x_b, y_b) and (x_e, y_e) also represent coordination of supporting leg tip B and swinging leg tip E, respectively. In the following, robot dynamics is obtained in SSP, DSP, double impact, and leg transpose matrix states.

2.1. Single Support Phase. The single support phase refers to the state where one leg is placed on the ground as support and another leg moves from back to the front, starting when the swinging tip leaves the ground, continuing until it reaches the ground. The point that the supporting leg contacts the ground is assumed a constant position. The robot dynamics is then calculated at the SSP state using the Lagrange method [42, 43]:

$$D(\theta)\ddot{\theta} + H(\theta, \dot{\theta})\dot{\theta} + G(\theta) = T_\theta, \tag{2}$$

where $D(\theta)$ is the 5×5 positive definite and symmetric matrix of inertia and $H(\theta, \dot{\theta})$ is a 5×5 matrix involving the terms of Coriolis and centrifugal forces of the robot. $G(\theta)$ is a 5×1 vector involving terms related to the gravity force felt by the robot, while $\theta, \dot{\theta}, \ddot{\theta}$, and T_θ are also 5×1 vectors for position, velocity, acceleration, and torque of the robot, respectively.

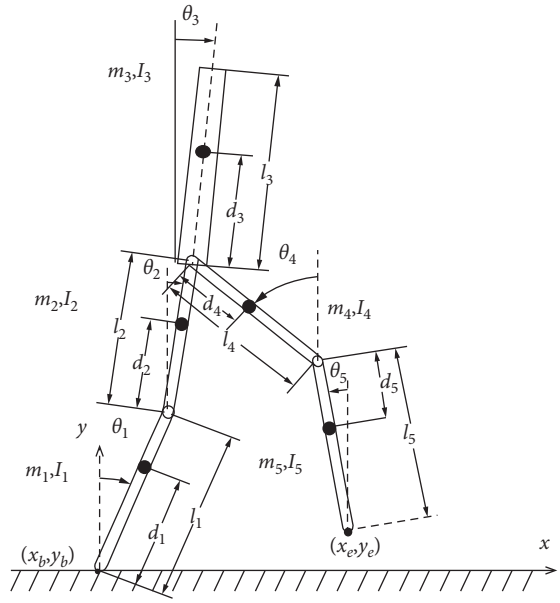

Figure 1: Five-link biped robot [42].

$$\begin{aligned} D &= \langle D_{ij} \rangle_{5\times5}, G = \langle G_{ij} \rangle_{5\times1}, H = \langle H_{ij} \rangle_{5\times5}, \\ D_{ij} &= p_{ij} \cos\left(\theta_i - \theta_j\right), \\ H_{ij} &= p_{ij} \sin\left(\theta_i - \theta_j\right)\dot{\theta}_j, \\ G_i &= g_i \sin\left(\theta_i\right), \end{aligned} \tag{3}$$

where $i, j = 1, 2, ..., 5$, p_{ij}, and g_i are defined as below and $a_i = \begin{cases} 0 & i = 3 \\ 1 & i \neq 3 \end{cases}$:

$$\begin{aligned} p_{ij} &= \begin{cases} I_i + m_i d_i^2 + a_i \left(\sum_{k=i+1}^{5} m_k \right) l_i^2 & j = i \\ a_i m_j d_j l_i + a_i a_j \left(\sum_{k=i+1}^{5} m_k \right) l_i l_j & j > i \\ p_{ji} & j < i \end{cases}, \\ g_i &= m_i d_i g + a_i \left(\sum_{k=i+1}^{5} m_k \right) l_i g, \end{aligned} \tag{4}$$

2.2. Double Support Phase. Both legs are placed on the ground in the double support phase state, and the trunk can move forward moderately. This state begins when the swinging leg touches the ground ending with the rear leg detaching from the ground. Since both legs are fixed on the ground in this state, some constraints were incorporated into the robot dynamics, known as Holonomic constraints [42, 43]:

$$\Phi(\theta) = \begin{bmatrix} f_1 \\ f_2 \end{bmatrix} = \begin{bmatrix} x_e - x_b - L \\ y_e - y_b \end{bmatrix} = 0, \tag{5}$$

where L is the distance between the tips of the robot. Then, in order to be applied in the dynamic derivation, they are differentiated twice concerning time; thus

$$\begin{aligned}\dot{\Phi}(\theta) &= J(\theta)\dot{\theta} = 0,\\ \ddot{\Phi}(\theta) &= \dot{J}(\theta)\dot{\theta} + J(\theta)\ddot{\theta} = 0,\end{aligned} \tag{6}$$

where J is a 2×5 Jacobian matrix.

$$J(\theta) = \begin{bmatrix} l_1\cos(\theta_1) & l_2\cos(\theta_2) & 0 & l_2\cos(\theta_2) & l_5\cos(\theta_5) \\ -l_1\sin(\theta_1) & -l_2\sin(\theta_2) & 0 & l_4\sin(\theta_4) & l_5\sin(\theta_5) \end{bmatrix}. \tag{7}$$

Using the Lagrange equation and Lagrange coefficients, the robot dynamics in the DSP state would be

$$D(\theta)\ddot{\theta} + H(\theta,\dot{\theta})\dot{\theta} + G(\theta) = J^T(\theta)\lambda + T_\theta, \tag{8}$$

where D, H, G, and T_θ are like terms expressed previously and λ is a 2×1 vector containing Lagrange coefficients. Next, λ was obtained from constraint conditions of the model. Considering the Jacobian not to be a square matrix, calculating the multipliers directly was impossible. In this regard, $J(\theta)D^{-1}(\theta)$ were multiplied by both sides of the DSP equation:

$$\begin{aligned}&J(\theta)\ddot{\theta} + J(\theta)D^{-1}(\theta)(H(\theta,\dot{\theta})\dot{\theta} + G(\theta))\\ &= \left(J(\theta)D^{-1}(\theta)J^T(\theta)\right)\lambda + J(\theta)D^{-1}(\theta)T_\theta.\end{aligned} \tag{9}$$

Herein, $J(\theta)\ddot{\theta} = -\dot{J}(\theta)\dot{\theta}$: thus, $J(\theta)D^{-1}(\theta)J^T(\theta)$ is invertible due to being a 2×2 matrix and positive definite, as well as $D(\theta)$ being of rank 5 surrounding the operating point. Now, λ can be calculated. $J(\theta)D^{-1}(\theta)J^T(\theta)$ is the pseudo-Jacobian matrix. In cases with unavailable invertible Jacobian matrices, it would help solve inverse kinematics. Finally, below are the DSP dynamic equations:

$$\begin{aligned}\ddot{\theta} &= D^{-1}(\theta)\left(T_\theta - (H(\theta,\dot{\theta})\dot{\theta} + G(\theta)) + J^T(\theta)\lambda\right)\\ \lambda &= -\left(J(\theta)D^{-1}(\theta)J^T(\theta)\right)^{-1}\\ &\quad\times\left(J(\theta)D^{-1}(\theta)\left(T_\theta - (H(\theta,\dot{\theta})\dot{\theta} + G(\theta))\right) + \dot{J}(\theta)\dot{\theta}\right).\end{aligned} \tag{10}$$

For more details, see [42, 43].

2.3. Impact Mapping. As soon as the robot leg contacts the ground, the impact occurs momentarily. Impacts make the velocity of robot joints change immediately. The impact can occur in different forms depending on the robot dynamics, materials employed for robot links, and roughness of the ground surface. Conventionally, the impact is assumed to occur between two rigid masses as a plastic impact within an insignificant time. The impact can occur at both single or double support phases. Single impact occurs when the supporting leg detaches from the ground just when the swinging leg reaches the ground. The supporting leg is still on the ground in the double impact when the swinging leg touches the ground. The present study has considered double impact cases. The impact can be assessed based on Newton's impact theory and the survival principle of linear and angular momentum for impact and torque. Assuming that velocities of contact points are zero immediately after impact and these two points do not slip or move up, the impact map for the intended biped robot can be expressed as

$$\dot{\theta}^+ = \dot{\theta}^- + D^{-1}(\theta)J^T(\theta)\left(J(\theta)D^{-1}(\theta)J^T(\theta)\right)^{-1}(-v_e^-), \tag{11}$$

where $\dot{\theta}^-$ and $\dot{\theta}^+$ are velocity vectors before and after the contact time, respectively, and $v_e^- = J(\theta)\dot{\theta}^-$ is the velocity of the swinging leg tip just before the contact time. As an assumption, the position vector does not change under the influence of impact.

2.4. Transformation Mapping. The motion starts from the double support phase, followed by the single support phase. When the swinging leg reaches the ground, the single support phase ends to map the impact, and the double support phase starts subsequently. Therefore, the robot has stepped down once. After the single support phase, the robot enters the double support phase. The cycle is repeated. Accordingly, the supporting leg at the previous phase switches to the swinging leg, and the swinging leg at the previous phase switches to the supporting leg in the new step. Robot dynamics equations are not changed in the new step, but a change can be observed in the role of joints and links. In this regard, a transformation is needed to express variables of the new step in terms of previous variables. The mapping would be then

$$\begin{pmatrix}\theta_{initial}\\ \dot{\theta}_{initial}\end{pmatrix} = \begin{pmatrix}T_{Switch} & 0_{5\times5}\\ 0_{5\times5} & T_{Switch}\end{pmatrix}\begin{pmatrix}\theta^-\\ \dot{\theta}^+_{\mathrm{Im}pact}\end{pmatrix}$$
$$T_{Switch} = \begin{bmatrix}0 & 0 & 0 & 0 & -1\\ 0 & 0 & 0 & -1 & 0\\ 0 & 0 & 1 & 0 & 0\\ 0 & -1 & 0 & 0 & 0\\ -1 & 0 & 0 & 0 & 0\end{bmatrix}. \tag{12}$$

where $\begin{bmatrix}\theta_{initial} & \dot{\theta}_{initial}\end{bmatrix}^T$ is a vector for initial variables of the new step, which is transformed to $\begin{bmatrix}\theta^- & \dot{\theta}^+_{Impact}\end{bmatrix}^T$, the vector of robot variables at final moment in the previous step, just after impact mapping [42, 43].

3. Motion Planning

Designing the trajectory is a crucial step in developing biped robot motions. During the movement, the trunk has a balance, and the movement of the thigh ending directly and horizontally influences the maintaining of the dynamical balance of walking substantially. Several important issues related to trajectory design have been addressed in previous research. Most related studies focus on trajectory design within SSP, putting less emphasis on DSP. DSP motion has an essential role in fast motion and balance maintenance. Furthermore, motion plans should contain both SSP and DSP states: this smooth trajectory design eliminates impact-

driven velocity changes. It also helps select trajectory design parameters to maintain stability [42, 43].

T_D is the time for DSP and T_s represents the time for movement in the SSP phase. The role of rotating and stance limbs is exchanged during walking. Regarding real human walking, the movement of the trunk remains directly upturned or swings directly around a specific point. It has been recommended to consider $\theta_3(t) = 0$ for both SSP and DSP states. Herein, the main task is to combine the motion of lower limbs. To satisfy the real walking equations, it is natural that initially the trajectory is designed for the rotating limb tip (foot), followed by designing a trajectory for the thigh. The final coordination of limbs has been exhibited in the form of X_a: $(x_a(t), y_a(t))$ vector relative to the absolute coordinate. The polynomial functions for the final point are expressed as follows:

$$X_a: \begin{cases} x_a = a_0 + a_1 t + a_2 t^2 + a_3 t^3 & 0 \le t \le T_S \\ y_a = b_0 + b_1 t + b_2 t^2 + b_3 t^3 + b_4 t^4 + b_5 t^5 & 0 \le t \le T_S \end{cases} \tag{13}$$

Equations of these constraints have been obtained according to conditions of trajectory design. Four major values denote the motion of a biped robot: the step's length SL, the SSP time period T_s, the maximum height of rising the leg H_m, and its position S_m, as well as the time needed to reach the maximum height T_m. These values are designed based on motion demands, while other values are designed following the demand for repeatability and continuity. These constraints are as follows:

(1) Geometrical constraints: the robot's feet should initially leave the ground and ultimately contact the ground again $y_a(0) = 0, y_a(T_s) = 0$.

(2) The maximum height of rising the leg: feet must have a distance from the ground to avoid any impact during walking.

$$x_a(T_m) = S_m, y_a(T_m) = H_m, \dot{y}_a(T_m) = 0. \tag{14}$$

(3) Motion repeatability: the initial state and velocities must be equal at the end of each step in DSP. Also, the initial and final steps should be equal for state repeatability. Therefore, robot feet touch the ground and remain fixed during DSP. The repeatability of velocity in the next cycle would be achievable when the initial velocity of feet remains zero in both vertical and horizontal directions.

$$\begin{aligned} x_a(0) &= -\frac{S_L}{2}; x_a(T_s) = \frac{S_L}{2} \\ \dot{x}_a(0) &= 0; \dot{y}_a(0) = 0. \end{aligned} \tag{15}$$

(4) Motion continuity: the final state of SSP and the initial state of DSP should be continuous. To foster the conditions for continuity, the velocity of the final point should reach zero immediately. However, the impact occurs when the robot's feet touch the ground leading to a sudden change in the joint angular velocity. The lower velocity at the final point causes a lower impact. Assuming the velocity of the final point before the impact is equal to zero, a sudden jump in the angular velocity is omitted, leading to $\dot{x}_a(T_s) = 0, \dot{y}_a(T_s) = 0$. These equations can be used in polynomials to solve unknown terms and conduct a repeatable motion with no effect from the impact.

The thigh movement has a considerable effect on the stability of the biped robot. The trajectory design for the thigh has been performed separately for SSP and DSP with coordination of X_{hS}: $(x_{hS}(t), y_{hS}(t))$ and X_{hD}: $(x_{hD}(t), y_{hD}(t))$, respectively.

$$\begin{aligned} X_{hS}: &\begin{cases} x_{hS} = c_0 + c_1 t + c_2 t^2 + c_3 t^3 & 0 \le t \le T_s \\ y_{hS} = y_h(t) & 0 \le t \le T \end{cases} \\ X_{hD}: &\begin{cases} x_{hD} = d_0 + d_1 t + d_2 t^2 + d_3 t^3 & 0 \le t \le T_D. \\ y_{hD} = y_h(t) & 0 \le t \le T_D \end{cases} \end{aligned} \tag{16}$$

The next section presents the case in which there are some constraints imposed on the position of the thigh at the start of SSP (S_{S0}) and DSP (S_{D0}) and the time of motion in SSP (T_D), and the height of the thigh (H_h). Herein, the motion is stable during DSP in addition to continuity and repeatability. Constraining cases are as follows:

(1) Vertical thigh movement: one characteristic of the movement in biped robots is the insubstantial vertical movement in the robot's center of mass which requires decreasing thigh vertical movement. y_{hS} and y_{hD} were considered to be constant during the motion in order to motion simplification $y_{hS}(t) = H_h, y_{hD}(t) = H_h$.

(2) Motion repeatability: it is maintained when the known triangle of the thigh and two ending limbs are the same at the start of SSP and end of DSP. Thus, the velocity of the thigh must be constant at both the beginning and end of each walking step. The following equations must then be observed:

$$\begin{aligned} x_{hS}(0) &= -S_{S0}; x_{hD}(T_D) = \frac{S_L}{2} - S_{S0}, \\ \dot{x}_{hS}(0) &= V_{h1}; \dot{x}_{hD}(T_D) = V_{h1}, \end{aligned} \tag{17}$$

where V_{h1} is the velocity of the thigh at the beginning of each step.

(3) Motion continuity: design of the thigh trajectory must be continuous along the motion trajectory. Horizontal velocity and position of thigh must be the same at the start of SSP and end of DSP.

$$\begin{aligned} x_{hS}(T_S) &= S_{D0}; \quad x_{hD}(0) = S_{D0}, \\ \dot{x}_{hS}(T_S) &= V_{h2}; \quad \dot{x}_{hD}(0) = V_{h2}. \end{aligned} \tag{18}$$

where V_{h2} is the velocity of the thigh at the end of each step.

The joint angle profile can be determined using the thigh and shank motion trajectory design and the biped robot kinematics model [42, 43].

$$\theta_1(t) = \arcsin\left(\frac{A_1C_1 + B_1\sqrt{A_1^2 + B_1^2 - C_1^2}}{A_1^2 + B_1^2}\right)$$

$$\theta_2(t) = \theta_1(t) + \arcsin\left(\frac{A_1\cos(\theta_1(t)) - B_1\sin(\theta_1(t))}{l_2}\right)$$

$$\theta_3(t) = 0,$$

$$\theta_4(t) = \arcsin\left(\frac{A_4C_4 + B_4\sqrt{A_4^2 + B_4^2 - C_4^2}}{A_4^2 + B_4^2}\right)$$

$$\theta_5(t) = \theta_4(t) + \arcsin\left(\frac{A_5\cos(\theta_5(t)) - B_5\sin(\theta_5(t))}{l_5}\right). \tag{19}$$

That would be for SSP:

$$\begin{aligned} A_1 &= x_{hS}(t); B_1 \\ C_1 &= \frac{A_1^2 + B_1^2 + l_1^2 - l_2^2}{2l_1} \\ A_4 &= x_{aS}(t) - x_{hS}(t) \\ B_4 &= y_{hS}(t) - y_{aS}(t) \\ C_4 &= \frac{A_4^2 + B_4^2 + l_4^2 - l_5^2}{2l_4}, \end{aligned} \tag{20}$$

and for DSP:

$$\begin{aligned} A_1 &= x_{hD}(t); \quad B_1 = y_{hD}(t) \\ C_1 &= \frac{A_1^2 + B_1^2 + l_1^2 - l_2^2}{2l_1} \\ A_4 &= \frac{S_L}{2} - x_{hD}(t); B_4 = y_{hD}(t) \\ C_4 &= \frac{A_4^2 + B_4^2 + l_4^2 - l_5^2}{2l_4}. \end{aligned} \tag{21}$$

It should be noted that the joint angles are considered limited as $-1 \le \theta_1 \le 1, -1.4 \le \theta_2 \le 0.7, -0.1 \le \theta_3 \le 0.1, -1 \le \theta_4 \le 1.5, -1.5 \le \theta_5 \le 1$, where numbers are based on radian.

4. Adaptive Nonsingular Fast Terminal Sliding Mode Controller Design

4.1. ANFTSM Design for SSP. The SSP dynamic equation for a biped robot can be written as

$$D(\theta)\ddot{\theta} + H(\theta, \dot{\theta})\dot{\theta} + G(\theta) = T_\theta + T_d, \tag{22}$$

where $D(\theta) = D_0(\theta) + \Delta D(\theta)$, $H(\theta, \dot{\theta}) = H_0(\theta, \dot{\theta}) + \Delta H(\theta, \dot{\theta})$, and $G(\theta) = G_0(\theta) + \Delta G(\theta)$. Nominal values are $D_0(\theta)$, $H_0(\theta, \dot{\theta})$, and $G_0(\theta)$, and perturbations of the system are represented by $\Delta D(\theta)$, $\Delta H(\theta, \dot{\theta})$, and $\Delta G(\theta)$. T_d is also the torque vector for the external perturbation. Now, the system defined in (22) can be expressed as

$$D_0(\theta)\ddot{\theta} + H_0(\theta, \dot{\theta})\dot{\theta} + G_0(\theta) = T_\theta + \varphi_d(\theta, \dot{\theta}, \ddot{\theta}), \tag{23}$$

where the lumped disturbance; i.e., $\varphi_d(\theta, \dot{\theta}, \ddot{\theta}) = T_d - \Delta D(\theta)\ddot{\theta} - \Delta H(\theta, \dot{\theta})\dot{\theta} - \Delta G(\theta)$ includes system perturbations and the external disturbance.

The present paper designed a robust controller to achieve fast convergence and precise tracking. Accordingly, system (27) has been considered by imposing the following conditions.

Assumption 1. The inertia matrix $D(\theta)$ is bounded at all θ still in the presence of uncertainty.

Assumption 2. The upper bound for the lumped perturbation is

$$\left|\varphi_d(\theta, \dot{\theta}, \ddot{\theta})\right| < \delta_1 + \delta_2|\theta| + \delta_3|\dot{\theta}|^2, \tag{24}$$

where $\delta_1, \delta_2, \delta_3$ are positive unknown constants.

If θ_d is the intended vector of position, the tracking error and its derivatives are $e = \theta - \theta_d$ and $\dot{e} = \dot{\theta} - \dot{\theta}_d$, respectively; thus

$$\begin{aligned} e &= D_0^{-1}(\theta)\left(T_\theta - \left(H_0(\theta, \dot{\theta})\dot{\theta} + G_0(\theta)\right) + \varphi_d(\theta, \dot{\theta}, \ddot{\theta})\right) \\ -\theta_d &= -D_0^{-1}(\theta)\left(H_0(\theta, \dot{\theta})\dot{\theta} + G_0(\theta)\right) - \ddot{\theta}_d \\ &\quad + D_0^{-1}(\theta)T_\theta + \varphi(\theta, \dot{\theta}, \ddot{\theta}). \end{aligned} \tag{25}$$

$\varphi(\theta, \dot{\theta}, \ddot{\theta}) = D_0^{-1}(\theta)\varphi_d(\theta, \dot{\theta}, \ddot{\theta})$. Applying Assumptions 1 and 2 in (24) leads to

$$|\varphi(\theta, \dot{\theta}, \ddot{\theta})| < \overline{\delta}_1 + \overline{\delta}_2|\theta| + \overline{\delta}_3|\dot{\theta}|^2, \tag{26}$$

where $\overline{\delta}_1, \overline{\delta}_2, \overline{\delta}_3$ are positive unknown constants. Herein, the robust controller of the system (23) was designed to investigate the reference trajectory tracking. Firstly, a nonlinear fast terminal sliding mode surface must be considered:

$$S = e + w_1|e|^\alpha sign(e) + w_2|\dot{e}|^\beta sign(\dot{e}). \tag{27}$$

Positive constants of w_1, w_2 are used while observing $\alpha > \beta$ and $1 < \beta < 2$. The derivative of (27) concerning time would be

$$\dot{S} = \dot{e} + \alpha w_1|e|^{\alpha-1}\dot{e} + \beta w_2|\dot{e}|^{\beta-1}\ddot{e}. \tag{28}$$

The control law of joint torque T_θ consists of two terms: the equivalent control and auxiliary control.

$$T_\theta = T_\theta^{eq} + T_\theta^{au}. \tag{29}$$

With $\varphi(\theta, \dot{\theta}, \ddot{\theta}) = 0$ and $\dot{S} = 0$, (32) might lead to T_θ^{eq} while T_θ^{au} deals with perturbations and system uncertainties. Both T_θ^{eq} and T_θ^{au} designing are represented in the following:

$$T_\theta^{eq} = D_0(\theta)\ddot{\theta}_d + H_0(\theta,\dot{\theta})\dot{\theta} + G_0(\theta) - \frac{1}{\beta w_2} D_0(\theta)|\dot{e}|^{2-\beta}\left(1 + \alpha w_1 |e|^{\alpha-1}\right) sign(\dot{e})$$

$$T_\theta^{au} = -D_0(\theta)\left(wS + \left(\hat{\bar{\delta}}_1 + \hat{\bar{\delta}}_2|\theta| + \hat{\bar{\delta}}_3|\dot{\theta}|^2 + \xi\right) sign(S)\right), \tag{30}$$

where ξ and w are small positive constant and positive definite matrix, respectively. $\hat{\bar{\delta}}_i, i = 1,2,3$ represent the estimates of $\bar{\delta}_i, i = 1,2,3$ with the following adaptive laws:

$$\begin{aligned} \dot{\hat{\bar{\delta}}}_1 &= \varepsilon_1 |S||\dot{e}|^{\beta-1}, \\ \dot{\hat{\bar{\delta}}}_2 &= \varepsilon_2 |S||\dot{e}|^{\beta-1}|\theta|, \\ \dot{\hat{\bar{\delta}}}_3 &= \varepsilon_3 |S||\dot{e}|^{\beta-1}|\dot{\theta}|^2. \end{aligned} \tag{31}$$

Herein, $\varepsilon_i, i = 1,2,3$ are positive constants.

Theorem 1. *For the unknown nonlinear SSP dynamic (27), the sliding mode surface can be attained in finite time by tracking error dynamics, followed by asymptotic convergence to zero through a nonlinear fast terminal sliding mode (31), control laws (33) and (34), and the adaptive law (35).*

Proof. Adaptation error can be defined as $\tilde{\bar{\delta}}_i = \hat{\bar{\delta}}_i - \bar{\delta}_i, i = 1,2,3$ and according to the following Lyapunov function candidate:

$$V = \frac{1}{2}\left(S^T S + \beta w_2 \left(\frac{1}{\varepsilon_1}\tilde{\bar{\delta}}_1^2 + \frac{1}{\varepsilon_2}\tilde{\bar{\delta}}_2^2 + \frac{1}{\varepsilon_3}\tilde{\bar{\delta}}_3^2\right)\right). \tag{32}$$

The time derivative of V would be

$$\dot{V} = S^T\dot{S} + \beta w_2\left(\frac{1}{\varepsilon_1}\tilde{\bar{\delta}}_1\dot{\hat{\bar{\delta}}}_1 + \frac{1}{\varepsilon_2}\tilde{\bar{\delta}}_2\dot{\hat{\bar{\delta}}}_2\frac{1}{\varepsilon_3}\tilde{\bar{\delta}}_3\dot{\hat{\bar{\delta}}}_3\right). \tag{33}$$

Now, (32) is substituted into (37) to obtain

$$\dot{V} = S^T\left(\dot{e} + \alpha w_1|e|^{\alpha-1}\dot{e} + \beta w_2|\dot{e}|^{\beta-1}\ddot{e}\right) + \beta w_2\left(\frac{1}{\varepsilon_1}\tilde{\bar{\delta}}_1\dot{\hat{\bar{\delta}}}_1 + \frac{1}{\varepsilon_2}\tilde{\bar{\delta}}_2\dot{\hat{\bar{\delta}}}_2\frac{1}{\varepsilon_3}\tilde{\bar{\delta}}_3\dot{\hat{\bar{\delta}}}_3\right). \tag{34}$$

This derivative can be revised through substitution of error dynamics (29) and adaptive control laws (33) and (34) into the above equation:

$$\dot{V} = \beta w_2|\dot{e}|^{\beta-1}\left(\varphi(\theta,\dot{\theta},\ddot{\theta})S - wS^T S - \left(\hat{\bar{\delta}}_1 + \hat{\bar{\delta}}_2|\theta| + \hat{\bar{\delta}}_3|\dot{\theta}|^2 + \xi\right)|S|\right) + \beta w_2\left(\frac{1}{\varepsilon_1}\tilde{\bar{\delta}}_1\dot{\hat{\bar{\delta}}}_1 + \frac{1}{\varepsilon_2}\tilde{\bar{\delta}}_2\dot{\hat{\bar{\delta}}}_2\frac{1}{\varepsilon_3}\tilde{\bar{\delta}}_3\dot{\hat{\bar{\delta}}}_3\right). \tag{35}$$

Update of laws (35) leads to

$$\dot{V} = \beta w_2|\dot{e}|^{\beta-1}\left(\varphi(\theta,\dot{\theta},\ddot{\theta})S - wS^T S - \left(\hat{\bar{\delta}}_1 + \hat{\bar{\delta}}_2|\theta| + \hat{\bar{\delta}}_3|\dot{\theta}|^2 + \xi\right)|S|\right) + \beta w_2\left(\tilde{\bar{\delta}}_1|S||\dot{e}|^{\beta-1} + \tilde{\bar{\delta}}_2|S||\dot{e}|^{\beta-1}|\theta| + \tilde{\bar{\delta}}_3|S||\dot{e}|^{\beta-1}|\dot{\theta}|^2\right). \tag{36}$$

Now, (36) can be simplified as

$$\dot{V} = \beta w_2|\dot{e}|^{\beta-1}\left(\varphi(\theta,\dot{\theta},\ddot{\theta})S - wS^T S - \xi|S| - \left(\bar{\delta}_1 + \bar{\delta}_2|\theta| + \bar{\delta}_3|\dot{\theta}|^2\right)|S|\right). \tag{37}$$

Using (26) leads to the following inequality:

$$\begin{aligned} \dot{V} &\le \beta w_2|\dot{e}|^{\beta-1}\left(|\varphi(\theta,\dot{\theta},\ddot{\theta})||S| - wS^T S - \xi|S| - \left(\bar{\delta}_1 + \bar{\delta}_2|\theta| + \bar{\delta}_3|\dot{\theta}|^2\right)|S|\right) \\ &\le \beta w_2|\dot{e}|^{\beta-1}\left(-wS^T S - \xi|S|\right) \le 0. \end{aligned} \tag{38}$$

As $\dot{V} = 0$ occurs only when $S = 0$ is satisfied, using Barbalat's Lemma, it is concluded $\dot{V} < 0$ for $S \neq 0$ and $\dot{V} = 0$ only for $S = 0$. Thus, the Lyapunov stability theory guaranteed the asymptotic convergence of system states toward the sliding surface.

In Figure 2, the control diagram of the proposed method is shown. □

Remark 1. In order to show that the proposed controller has provided finite time, Lyapunov candidate $V_0 = (1/2)S^T S$ has been considered and by (42):

$$\dot{V}_0 \le \dot{V} + \tilde{\bar{\delta}}_1\dot{\hat{\bar{\delta}}}_1 + \tilde{\bar{\delta}}_2\dot{\hat{\bar{\delta}}}_2 + \tilde{\bar{\delta}}_3\dot{\hat{\bar{\delta}}}_3 \le \beta w_2|\dot{e}|^{\beta-1}\left(-wS^T S - \xi|S|\right) + \left(\hat{\bar{\delta}}_1 - \bar{\delta}_1\right)\dot{\hat{\bar{\delta}}}_1 + \left(\hat{\bar{\delta}}_2 - \bar{\delta}_2\right)\dot{\hat{\bar{\delta}}}_2 + \left(\hat{\bar{\delta}}_3 - \bar{\delta}_3\right)\dot{\hat{\bar{\delta}}}_3. \tag{39}$$

If $\bar{\delta}_i(0) < \hat{\bar{\delta}}_i(0), i = 1,2,3$ holds. Step 1: by using $\dot{\hat{\bar{\delta}}}_i \ge 0$, we have $T_1 \ge 0$ such that $\bar{\delta}_i(t) \ge \hat{\bar{\delta}}_i(t), i = 1,2,3, t \ge T_1$, which leads to $\dot{V}_0(t) \le \beta w_2|\dot{e}|^{\beta-1}(-wS^T S - \xi|S|)$, $t \ge T_1$. Step 2: otherwise, there is $T_2 \ge 0$ such that at least one $\dot{\hat{\bar{\delta}}}_i = 0$ and $\bar{\delta}_i(t) < \hat{\bar{\delta}}_i(t)$, $t \ge T_2$ that leads to $\dot{V}_0(t) \le \beta w_2|\dot{e}|^{\beta-1}(-wS^T S - \xi|S|) + (\hat{\bar{\delta}}_j - \bar{\delta}_j)\dot{\hat{\bar{\delta}}}_j + (\hat{\bar{\delta}}_k - \bar{\delta}_k)\dot{\hat{\bar{\delta}}}_k$, $j,k \neq i$, $t \ge T_2$. Then, we can use Step 1 or Step 2; thus, at last $\dot{V}_0(t) \le \beta w_2|\dot{e}|^{\beta-1}(-wS^T S - \xi|S|)$ in T_3 as finite time. If $\bar{\delta}_i(0) \ge \hat{\bar{\delta}}_i(0)$ for at least one of $i = 1,2,3$, one has $\bar{\delta}_i(t) \ge \hat{\bar{\delta}}_i(t), t \ge 0$, that is, $(\hat{\bar{\delta}}_i - \bar{\delta}_i)\dot{\hat{\bar{\delta}}}_i \le 0$. As for $\bar{\delta}_j(0) < \hat{\bar{\delta}}_j(0), j \neq i$ like to previous procedure it can obtain $\dot{V}_0(t) \le \beta w_2|\dot{e}|^{\beta-1}(-wS^T S - \xi|S|)$. Thus,

$$\dot{V}_0 \le \beta w_2|\dot{e}|^{\beta-1}\left(-wS^T S - \xi|S|\right) = -\rho_1 V_0 - \rho_2 V_0^{1/2}, \tag{40}$$

where $\rho_1 = 2w\beta w_2|\dot{e}|^{\beta-1} > 0, \rho_2 = \sqrt{2}\xi\beta w_2|\dot{e}|^{\beta-1} > 0$. Ultimately, there exists $t \ge T$ such that if $V_0 \le 1$, then $\dot{V}_0 \le -\rho_1 V_0 - \rho_2 V_0^{1/2} \le -(\rho_1 + \rho_2)V_0$, and if $V_0 > 1$, then $\dot{V}_0 \le -\rho_1 V_0 - \rho_2 V_0^{1/2} \le -(\rho_1 + \rho_2)V_0^{1/2}$. Thus, finite time can be provided by the proposed controller.

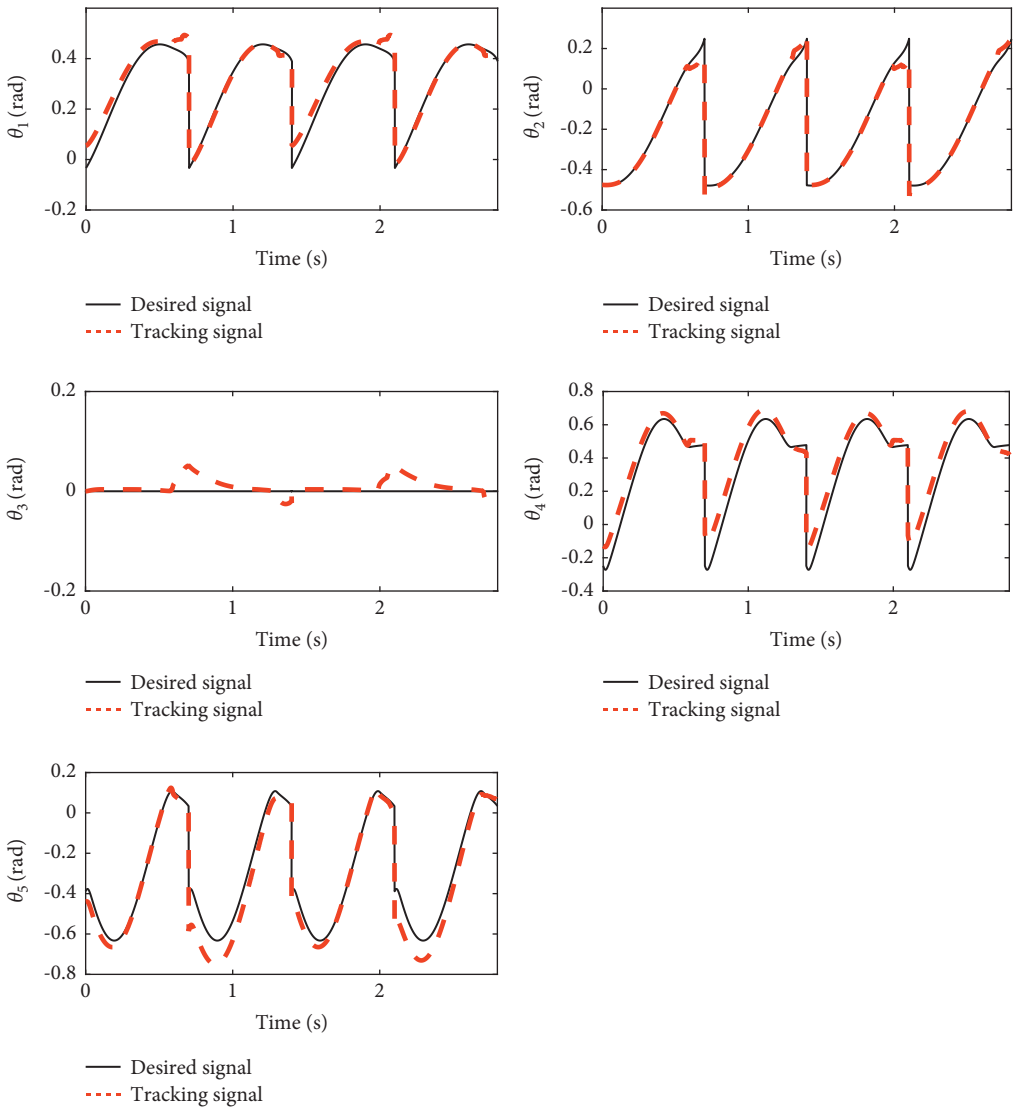

Figure 2: Joint angles.

4.2. ANFTSM Design for DSP. The DSP dynamic equation for biped robot can be written as

$$D(\theta)\ddot{\theta} + H(\theta,\dot{\theta})\dot{\theta} + G(\theta) = T_\theta + T_d + J^T(\theta)\lambda. \tag{41}$$

Considering the definition for J, λ,

$$\begin{aligned} D(\theta)\ddot{\theta} + H(\theta,\dot{\theta})\dot{\theta} + G(\theta) = {} & T_\theta + T_d \\ & - J^T(\theta)\left(J(\theta)D^{-1}(\theta)J^T(\theta)\right)^{-1} \\ & \times\left(J(\theta)D^{-1}(\theta)\left(T_\theta - (H(\theta,\dot{\theta})\dot{\theta}\right.\right. \\ & \left.\left. + G(\theta))\right) + \dot{J}(\theta)\dot{\theta}\right). \end{aligned} \tag{42}$$

The above relation can be rewritten as

$$\begin{aligned} & D(\theta)\ddot{\theta} + \left(I - L_1(\theta)L_2(\theta)\right)\left(H(\theta,\dot{\theta})\dot{\theta} + G(\theta)\right) \\ & \quad + L_1(\theta)\dot{J}(\theta)\dot{\theta}(\theta) \\ & = \left(I - L_1(\theta)L_2(\theta)\right)T_\theta + T_d. \end{aligned} \tag{43}$$

So that

$$\begin{aligned} L_1(\theta) &= J^T(\theta)\left(J(\theta)D^{-1}(\theta)J^T(\theta)\right)^{-1} \\ L_2(\theta) &= J(\theta)D^{-1}(\theta). \end{aligned} \tag{44}$$

Finally, (47) can be written as

$$D(\theta)\ddot{\theta} + h(\theta,\dot{\theta}) = \overline{T}_\theta + T_d, \tag{45}$$

where

$$h(\theta,\dot{\theta}) = \left(I - L_1(\theta)L_2(\theta)\right)\left(H(\theta,\dot{\theta})\dot{\theta} + G(\theta)\right) + L_1(\theta)\dot{J}(\theta)\dot{\theta}$$
$$\overline{T}_\theta = \left(I - L_1(\theta)L_2(\theta)\right)T_\theta. \tag{46}$$

Therefore, $\ddot{e}$ can be obtained in DSP state:

$$\begin{aligned}\ddot{e} &= D_0^{-1}(\theta)\left(\overline{T}_\theta - h(\theta,\dot{\theta}) + \overline{\varphi}_d(\theta,\dot{\theta},\ddot{\theta})\right) - \ddot{\theta}_d. \\ &= -D_0^{-1}(\theta)\left(h(\theta,\dot{\theta})\right) - \ddot{\theta}_d + D_0^{-1}(\theta)\overline{T}_\theta + \overline{\varphi}(\theta,\dot{\theta},\ddot{\theta}).\end{aligned} \tag{47}$$

We have $\overline{\varphi}_d(\theta,\dot{\theta},\ddot{\theta}) = T_d - \Delta D(\theta)\ddot{\theta} - \Delta h(\theta,\dot{\theta})$ and $\overline{\varphi}(\theta,\dot{\theta},\ddot{\theta}) = D_0^{-1}(\theta)\overline{\varphi}_d(\theta,\dot{\theta},\ddot{\theta})$. Thus, it can be assumed that

$$|\overline{\varphi}(\theta,\dot{\theta},\ddot{\theta})| < \overline{\mu}_1 + \overline{\mu}_2|\theta| + \overline{\mu}_3|\dot{\theta}|^2, \tag{48}$$

where $\overline{\mu}_1, \overline{\mu}_2, \overline{\mu}_3$ are positive unknown constants. The designs of $\overline{T}_\theta^{eq}$ and $\overline{T}_\theta^{au}$ are then expressed as

$$\begin{aligned}\overline{T}_\theta^{eq} &= D_0(\theta)\ddot{\theta}_d + h_0(\theta,\dot{\theta}) \\ &\quad - \frac{1}{\beta w_2}D_0(\theta)|\dot{e}|^{2-\beta}\left(1 + \alpha w_1|e|^{\alpha-1}\right)sign(\dot{e}) \\ \overline{T}_\theta^{au} &= -D_0(\theta)\left(wS + \left(\hat{\overline{\mu}}_1 + \hat{\overline{\mu}}_2|\theta| + \hat{\overline{\mu}}_3|\dot{\theta}|^2 + \xi\right)sign(S)\right) \\ \overline{T}_\theta &= \left(I - L_1(\theta)L_2(\theta)\right)^{-1}\left(\overline{T}_\theta^{eq} + \overline{T}_\theta^{au}\right).\end{aligned} \tag{49}$$

$\overline{\mu}_i, i = 1,2,3$ have the estimates $\hat{\overline{\mu}}_i, i = 1,2,3$ with respective adaptive laws as

$$\begin{aligned}\dot{\hat{\overline{\mu}}}_1 &= \varepsilon_1|S||\dot{e}|^{\beta-1}, \\ \dot{\hat{\overline{\mu}}}_2 &= \varepsilon_2|S||\dot{e}|^{\beta-1}|\theta|, \\ \dot{\hat{\overline{\mu}}}_3 &= \varepsilon_3|S||\dot{e}|^{\beta-1}|\dot{\theta}|^2.\end{aligned} \tag{50}$$

Theorem 2. *For an uncertain nonlinear DSP dynamic (45), the sliding mode surface can be attained in finite time by tracking error dynamics, followed by asymptotic convergence to zero through a nonlinear fast terminal sliding mode (31) as well as control and adaptive laws of (49) and (50), respectively. Proof of this theorem is the same as Theorem 1.*

Remark 2. For real applications, the control performance has been limited significantly due to significant difficulties deduced from the control engineering point of view: (i) recognizing the system model and determining the upper bound for the dynamical system uncertainties, (ii) the presence of system uncertainties as well as external perturbations, and (iii) the feasibility of control inputs. The proposed control scheme has required no detailed information about system dynamics and predetermined upper bounds. Additionally, the ANFTSM control with good efficacy has ensured robustness against perturbations and uncertainties. More importantly, real adaptive algorithm implementations of Theorems 1 and 2 are required to access position and velocity states for feedback. In the robot manipulator, each joint has been then equipped with a motor, an encoder, and a tachometer to provide input torque, measure joint position, and measure joint velocity, respectively. Therefore, practical implementation can be feasibly performed via control inputs with no harmful oscillation, namely, chattering. Consequently, the proposed controller has been promisingly suitable, particularly in practical applications, as shown in the next section.

Table 1: Robot parameters [43].

Link no.	m_i^0 (kg)	l_i (m)	d_i (m)	I_i^0 (m^3)
1	2.23	0.332	0.189	0.033
2	5.28	0.302	0.236	0.033
3	14.79	0.486	0.282	0.033
4	5.28	0.302	0.066	0.033
5	2.23	0.332	0.143	0.033

Table 2: Design parameters.

Parameter	α	β	ξ	w	w_1
SSP	2	5.3	0.01	95	1
DSP	2	1.9	0.01	115	1
Parameter	w_2	ε_1	ε_2	ε_3	
SSP	1	0.01	0.01	0.01	
DSP	1	0.01	0.01	0.01	

Remark 3. Increasing α and w_1 increased the effect of tracking error while increasing β and w_2 intensified the effect of the time derivative of tracking error in the sliding surface. Thus, it should be a tradeoff between the weights of the tracking error and its time derivative. Furthermore, in adaptation law, with increasing ε_i the speed of adaptation increases as well as the overshoot. Thus, it should be a tradeoff between a smooth and fast adaptation.

5. Simulation Results

This section presents the simulation results of ANFSM on the biped robot. The robot parameters are shown in Table 1.

The uncertainties in mass and inertia were considered 20% as $m_i = m_i^0 + 0.2m_i^0$, $I_i = I_i^0 + 0.2I_i^0$. Also, the robot carried a cargo $m_{\text{cargo}} = 5$kg suddenly at $t = 0.5s$ so, $m_3 = m_3 + m_{\text{cargo}}$ for $t \geq 0.5$. For external disturbances, a sudden force as $T_d = 5$ was considered for torso link at $t = 0.4s$. Parameters of motion trajectory were as $SL = 0.7m, T_S = 0.6s$, $T_D = 0.1s$, $X_m = (0, 0.05m)$, and the robot's velocity was 1 m/s. The initial conditions have been considered as $X_a(0)$: $(-0.3, 0)$, $X_h(0)$: $(-0.12, 0.6)$. Using inverse kinematic, the initial conditions of joints and angles have been calculated as $\theta(0) = [0.055, -0.4755, 0, -0.01291, -0.4390]^T$rad and $\dot{\theta}(0) = [0,0,0,0,0]^T$rad/s. The design parameters of the controller are shown in Table 2.

Figures 2–4 show the joint angles, tracking errors, and angular velocities. The angles could track their trajectories, and the tracking errors were tolerable with the existing uncertainties and external disturbances. Figure 5 displays the dynamic walking of the biped robot. The robot could walk at 1 m/s speed with guaranteed balance. Figure 6 shows

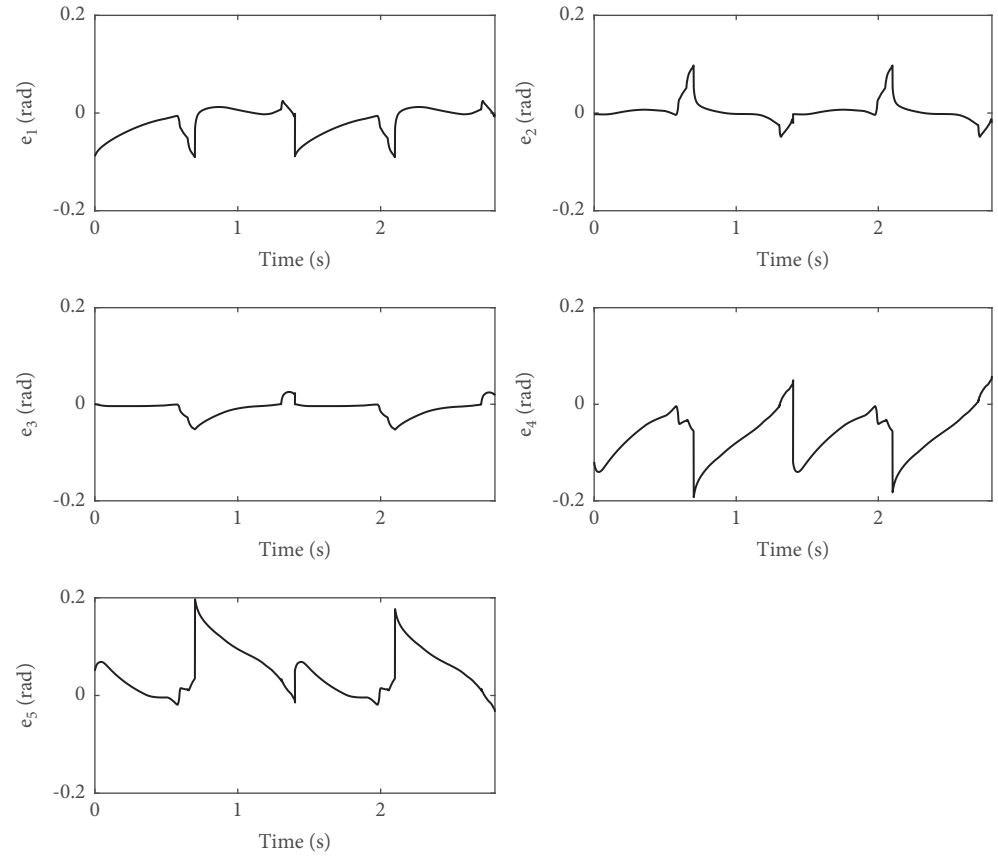

Figure 3: Tracking errors of joint angles.

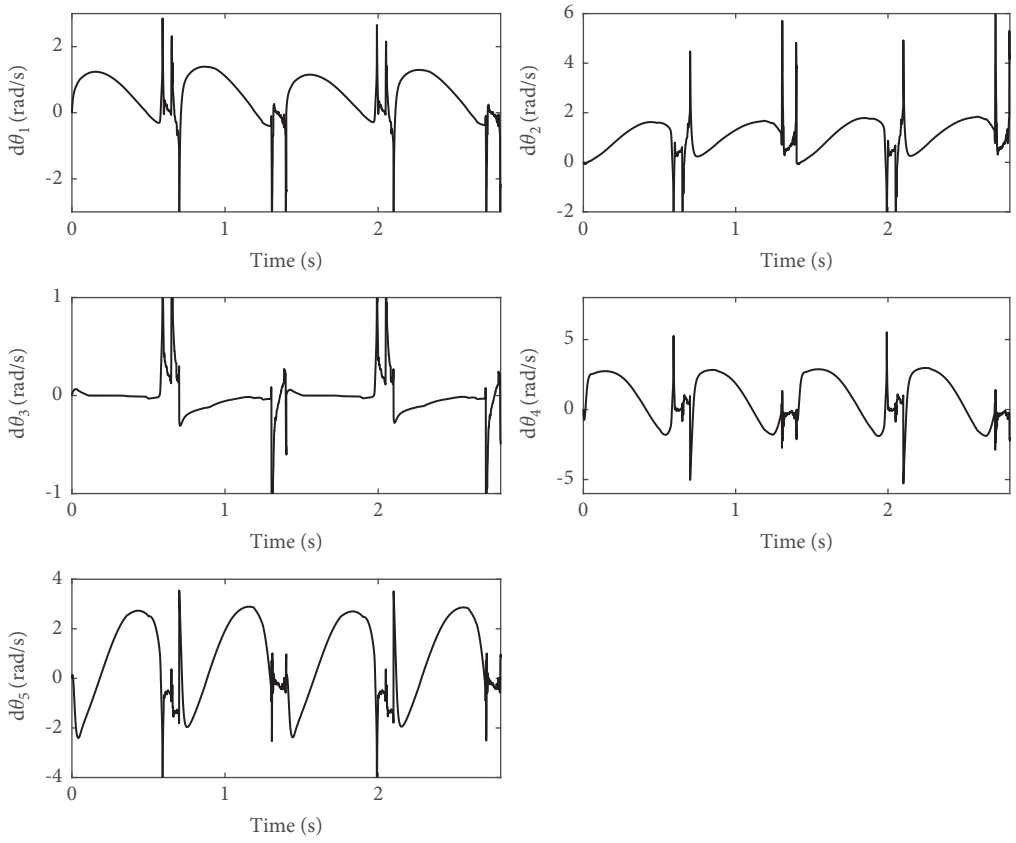

Figure 4: Angular velocities.

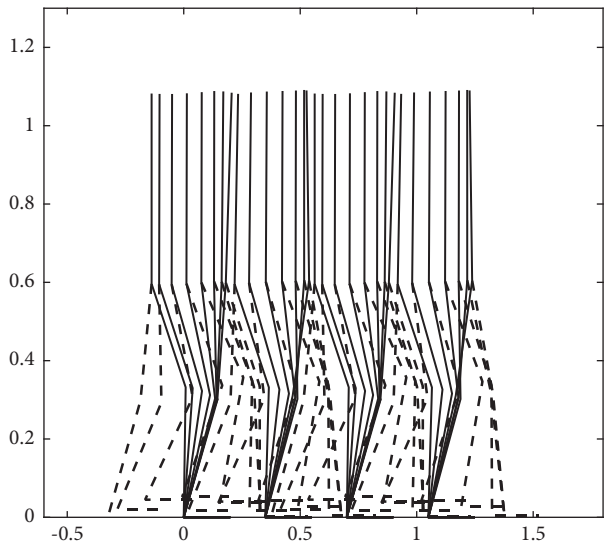

Figure 5: Dynamic walking.

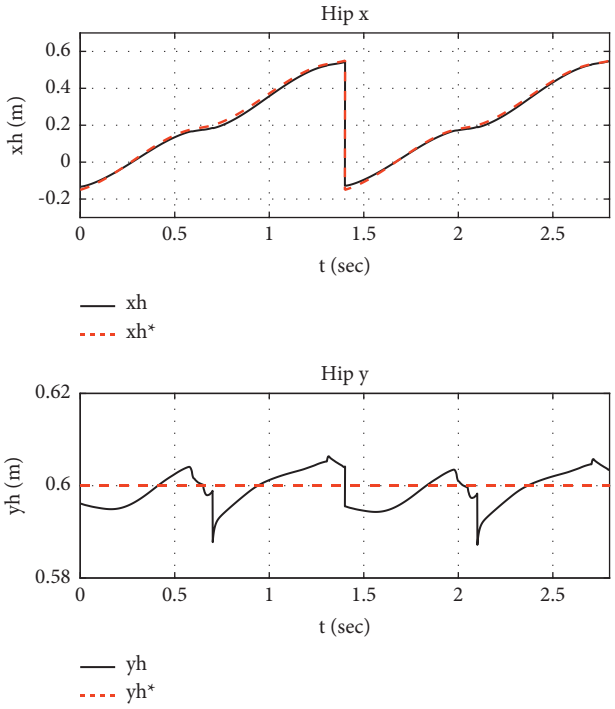

Figure 6: Tracking of hip.

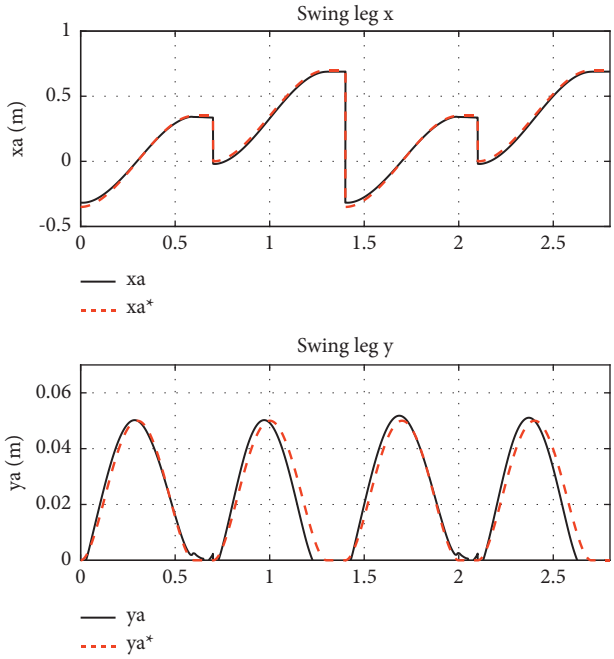

Figure 7: Tracking of swinging leg.

the hip position in x and y directions. The hip moved very smoothly in the x-direction. The error of hip in y-direction was less than 1 cm. Figure 7 demonstrates the swinging leg position. The hip tracked its trajectories in x and y directions with negligible error. The sliding surfaces are shown in Figure 8. The surfaces were converged to zero fast enough. The joint torques are shown in Figure 9. All torques were within their allowable limits. Also, in Table 3, the integral square errors and torques are shown.

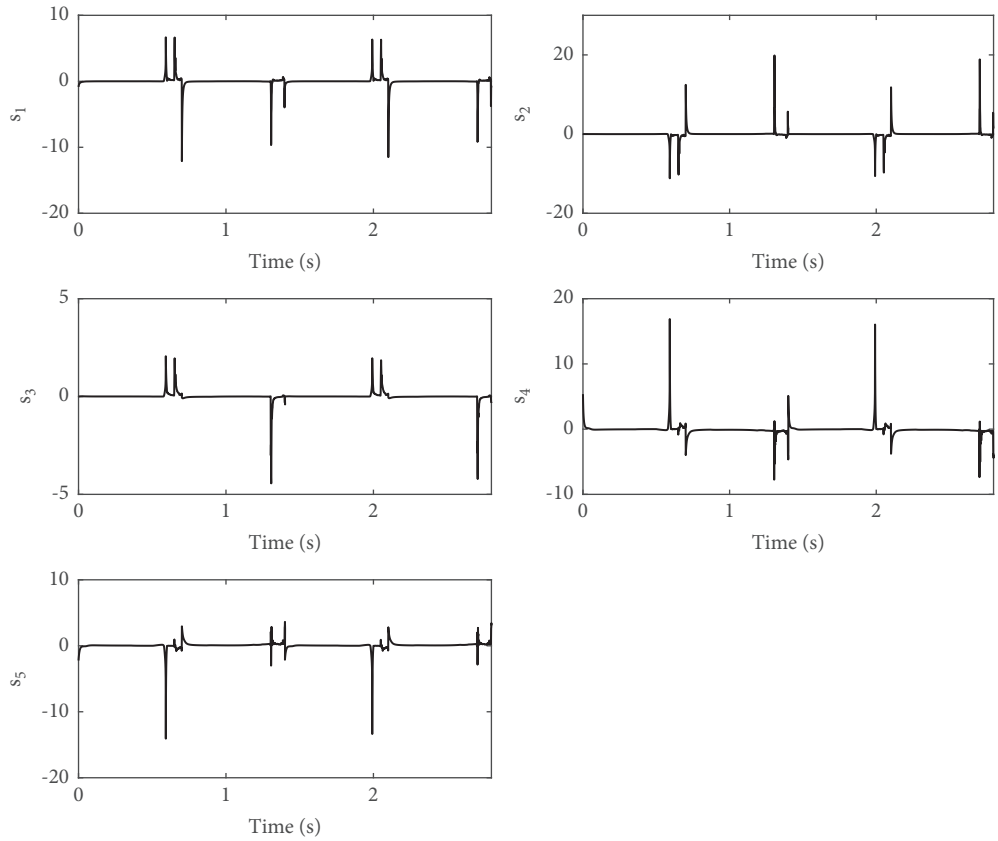

Figure 8: Sliding surfaces.

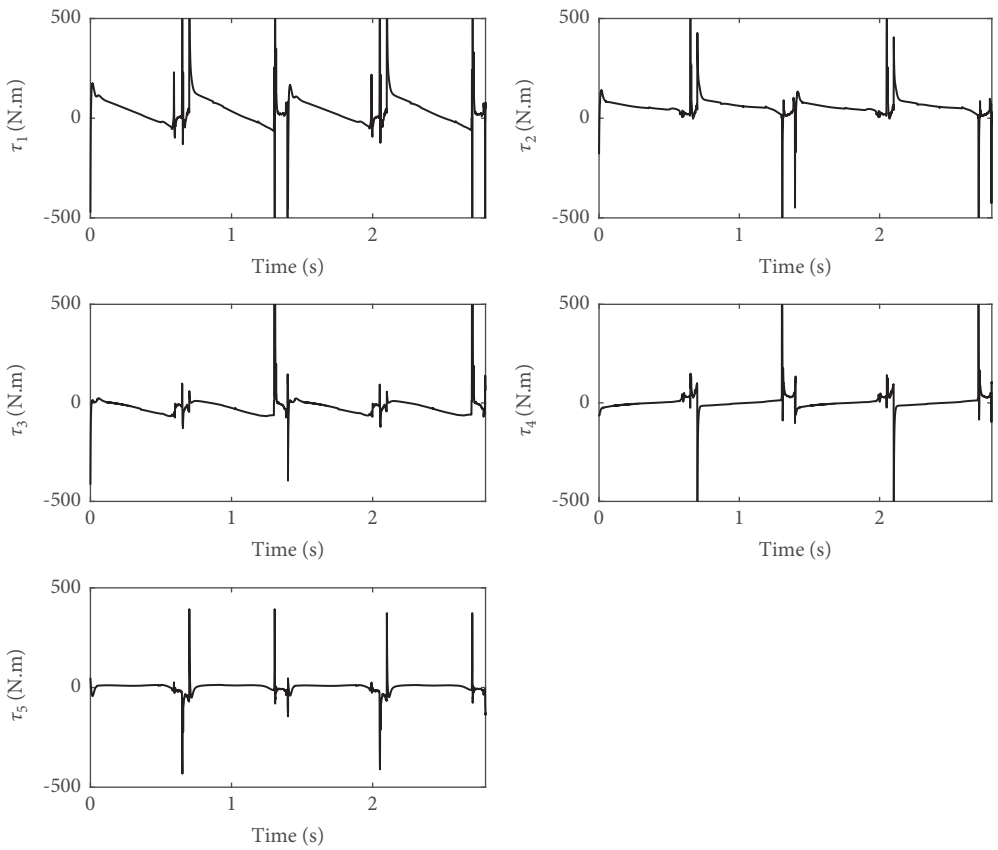

Figure 9: Joint torques.

Table 3: ISE for tracking errors and input signal.

	e_1	e_2	e_3	e_4	e_5
ISE	0.0834	0.0053	6.7×10^{-4}	2.9821	0.375
	τ_1	τ_2	τ_3	τ_4	τ_5
ISE	8.87×10^8	6.66×10^8	5.33×10^6	1.04×10^7	2.25×10^6

6. Conclusion

The present study has proposed an adaptive nonsingular fast terminal sliding mode control approach to control and maintain dynamic walking stability in a biped robot. The intended robot was a five-link planar robot to be examined under the uncertainty at both SSP and DSP states and external perturbations such as overloading and sudden impacts. The upper bound of uncertainty can be estimated online through designing an adoption law instead of using a predetermined value for this parameter. The proposed controller confirmed fast, robust, and stable tracking of the biped robot's dynamic movement on a smooth surface. Regarding three SSP, DSP, double impact states, and fast movement, robot behavior was closer to human behavior. The designed reference trajectories also confirmed the ZMP stability and maintained continuity. Simulation results proved the method's suitable performance in fast and robust tracking of reference trajectories of joints in the presence of uncertainty and external perturbation without predefined upper bounds.

In future research, three-dimensional movements and dynamic obstacle avoidance will be investigated. The time delays of control inputs will be added to the dynamic model, and the proposed method will be adapted against delays.

Data Availability

No data were used to support this study.

Conflicts of Interest

The authors declare that they have no conflicts of interest.

References

[1] A. Sabanovic, "Variable structure systems with sliding modes in motion control-A survey," *IEEE Transactions on Industrial Informatics*, vol. 7, no. 2, pp. 212–223, 2011.

[2] S. Ding, S. Li, and W. X. Zheng, "New approach to second-order sliding mode control design," *IET Control Theory & Applications*, vol. 7, no. 18, pp. 2188–2196, 2013.

[3] L. Zhao, H. Cheng, and T. Wang, "Sliding mode control for a two-joint coupling nonlinear system based on extended state observer," *ISA Transactions*, vol. 73, pp. 130–140, 2018.

[4] Y. Feng, X. Han, Y. Wang, and X. Yu, "Second-order terminal sliding mode control of uncertain multivariable systems," *International Journal of Control*, vol. 80, no. 6, pp. 856–862, 2007.

[5] D. Zhao, S. Li, and F. Gao, "A new terminal sliding mode control for robotic manipulators," *IFAC Proceedings Volumes*, vol. 41, no. 2, pp. 9888–9893, 2008.

[6] S. Ik Han and J. Lee, "Finite-time sliding surface constrained control for a robot manipulator with an unknown deadzone and disturbance," *ISA Transactions*, vol. 65, pp. 307–318, 2016.

[7] C.-S. Jeong, J.-S. Kim, and S.-I. Han, "Tracking error constrained super-twisting sliding mode control for robotic systems," *International Journal of Control, Automation and Systems*, vol. 16, no. 2, pp. 804–814, 2018.

[8] S. Mobayen, D. Baleanu, and F. Tchier, "Second-order fast terminal sliding mode control design based on LMI for a class of non-linear uncertain systems and its application to chaotic systems," *Journal of Vibration and Control*, vol. 23, pp. 1–14, 2017.

[9] J. Zhu and K. Khayati, "Adaptive sliding mode control - convergence and gain boundedness revisited," *International Journal of Control*, vol. 89, no. 4, pp. 801–814, 2016.

[10] J. Zhu and K. Khayati, "A new approach for adaptive sliding mode control: integral/exponential gain law," *Transaction of the Institute of Measurement and Control*, vol. 38, pp. 1–10, 2016.

[11] J. Zhu and K. Khayati, "On a new adaptive sliding mode control for MIMO nonlinear systems with uncertainties of unknown bounds," *International Journal of Robust and Nonlinear Control*, vol. 27, no. 6, pp. 942–962, 2017.

[12] Y. Huang, Z. Zheng, L. Sun, and M. Zhu, "Saturated adaptive sliding mode control for autonomous vessel landing of a quadrotor," *IET Control Theory & Applications*, vol. 12, no. 13, pp. 1830–1842, 2018.

[13] F. Plestan, Y. Shtessel, V. Brégeault, and A. Poznyak, "New methodologies for adaptive sliding mode control," *International Journal of Control*, vol. 83, no. 9, pp. 1907–1919, 2010.

[14] A. Nasiri, S. Kiong Nguang, and A. Swain, "Adaptive sliding mode control for a class of MIMO nonlinear systems with uncertainties," *Journal of the Franklin Institute*, vol. 351, no. 4, pp. 2048–2061, 2014.

[15] S. Roy, S. Bladi, and L. M. Fridman, "On adaptive sliding mode control without a priori bounded uncertainty," *Automatica*, vol. 111, Article ID 108650, 2019.

[16] H. Rabiee, M. Ataei, and M. Ekramian, "Continuous nonsingular terminal sliding mode control based on adaptive sliding mode disturbance observer for uncertain nonlinear systems," *Automatica*, vol. 109, pp. 1–7, 2019.

[17] Y. Miao, I. Hwang, M. Liu, and F. Wang, "Adaptive fast nonsingular terminal sliding mode control for attitude tracking of flexible spacecraft with rotating appendage," *Aerospace Science and Technology*, vol. 93, pp. 1–10, 2019.

[18] J.-Y. Zhai and Z.-B. Song, "Adaptive sliding mode trajectory tracking control for wheeled mobile robots," *International Journal of Control*, vol. 92, pp. 1–16, 2018.

[19] A. Goel and A. Swarup, "MIMO uncertain nonlinear system control via adaptive high-order super twisting sliding mode and its application to robotic manipulator," *Journal of Control, Automation and Electrical Systems*, vol. 28, no. 1, pp. 36–49, 2017.

[20] M. Boukattaya, N. Mezghani, and T. Damak, "Adaptive nonsingular fast terminal sliding-mode control for the tracking problem of uncertain dynamical systems," *ISA Transactions*, vol. 77, pp. 1–19, 2018.

[21] S. Yi and J. Zhai, "Adaptive second-order fast nonsingular terminal sliding mode control for robotic manipulators," *ISA Transactions*, vol. 90, pp. 41–51, 2019.

[22] M. Labbadi and M. Cherkaoui, "Robust adaptive nonsingular fast terminal sliding-mode tracking control for an uncertain quadrotor UAV subjected to disturbances," *ISA Transactions*, vol. 99, pp. 290–304, 2019.

[23] Z. Yan, M. Wang, and J. Xu, "Robust adaptive sliding mode control of underactuated autonomous underwater vehicles with uncertain dynamics," *Ocean Engineering*, vol. 173, pp. 802–809, 2019.

[24] D. Ashtiani Haghighi and S. Mobayen, "Design of an adaptive super-twisting decoupled terminal sliding mode control scheme for a class of fourth-order systems," *ISA Transactions*, vol. 75, pp. 216–225, 2018.

[25] S. Mobayen, F. Tchier, and L. Ragoub, "Design of an adaptive tracker forn-link rigid robotic manipulators based on super-twisting global nonlinear sliding mode control," *International Journal of Systems Science*, vol. 48, no. 9, pp. 1990–2002, 2017.

[26] J. Baek, M. Jin, and S. Han, "A new adaptive sliding-mode control scheme for application to robot manipulators," *IEEE Transactions on Industrial Electronics*, vol. 63, no. 6, pp. 3628–3637, 2016.

[27] A. Benamor and H. Messaoud, "Robust adaptive sliding mode control for uncertain systems with unknown time-varying delay input," *ISA Transactions*, vol. 79, pp. 1–12, 2018.

[28] D. Allahverdy, A. Fakharian, and M. B. Menhaj, "Back-stepping integral sliding mode control with iterative learning control algorithm for quadrotor UAVs," *Journal of Electrical Engineering & Technology*, vol. 14, no. 6, pp. 2539–2547, 2019.

[29] B. Barikbin and A. Fakharian, "Trajectory tracking for quadrotor UAV transporting cable-suspended payload in wind presence," *Transactions of the Institute of Measurement and Control*, vol. 41, no. 5, pp. 1243–1255, 2018.

[30] V. Azimi, M. B. Menhaj, and A. Fakharian, "Tool position tracking control of a nonlinear uncertain flexible robot manipulator by using robust H2/H∞ controller via T-S fuzzy model," *Sadhana*, vol. 40, no. 2, pp. 307–333, 2015.

[31] L. Qiao and W. Zhang, "Adaptive second-order fast nonsingular terminal sliding mode tracking control for fully actuated autonomous underwater vehicles," *IEEE Journal of Oceanic Engineering*, vol. 44, no. 2, pp. 363–385, 2019.

[32] L. Qiao and W. Zhang, "Trajectory tracking control of AUVs via adaptive fast nonsingular integral terminal sliding mode control," *IEEE Transactions on Industrial Informatics*, vol. 16, no. 2, pp. 1248–1258, 2020.

[33] L. Qiao and W. Zhang, "Double-loop integral terminal sliding mode tracking control for UUVs with adaptive dynamic compensation of uncertainties and disturbances," *IEEE Journal of Oceanic Engineering*, vol. 44, no. 1, pp. 29–53, 2019.

[34] S. Tzafestas, M. Raibert, and C. Tzafestas, "Robust sliding-mode control applied to a 5-link biped robot," *Journal of Intelligent and Robotic Systems*, vol. 15, no. 1, pp. 67–133, 1996.

[35] M. Nikkhah, H. Ashrafian, and F. Fahimi, "Sliding mode control of underactuated biped robots," in *Proceedings of the International Conference on Mechanical Engineering Congress and Exposition*, vol. 74, pp. 1361–1367, New York, NY, USA, February 2005.

[36] X. Mu and Q. Wu, "Development of a complete dynamic model of a planar five-link biped and sliding mode control of its locomotion during the double support phase," *International Journal of Control*, vol. 77, no. 8, pp. 789–799, 2004.

[37] S. A. A. Moosavian, A. Takhmar, and M. Alghooneh, "Regulated sliding mode control of a biped robot," in *Proceedings of the International Conference on Mechatronics and Automation*, pp. 1–6, Harbin, China, August 2007.

[38] H. Ghadiri, M. Emami, and H. Khodadadi, "Adaptive super-twisting non-singular terminal sliding mode control for tracking of quadrotor with bounded disturbances," *Aerospace Science and Technology*, vol. 112, Article ID 106616, 2021.

[39] L. Chen, Z. Liu, H. Gao, and G. Wang, "Robust adaptive recursive sliding mode attitude control for a quadrotor with unknown disturbances," *ISA Transactions*, 2021, (In Press).

[40] N. Kalamian and M. Farrokhi, "Dynamic walking of biped robots with obstacles using predictive controller," in *Proceedings of the International Conference on Computer and Knowledge Engineering*, pp. 160–165, Mashhad, Iran, October 2011.

[41] N. Kalamian and M. Farrokhi, "Stepping of biped robots over large obstacles using NMPC controller," in *Proceedings of the International Conference on Control, Instrumentation and Automation*, pp. 917–922, Shiraz, Iran, December 2011.

[42] X. Mu and Q. Wu, "A complete dynamic model of five-link bipedal walking," in *Proceedings of the - American Control Conference*, pp. 1–6, Denver, CO, USA, June 2003.

[43] X. Mu, *Dynamics and Motion Regulation of a Five-Link Biped Robot Walking in the Sagittal Plane*, PhD Dissertation, Department of Mechanical and Manufacturing Engineering, University of Manitoba, Manitoba, Canada, 2004.